

## Impact of Anionic Dopant Precursor on Nanostructured ZnO thin Films Surface Morphologies

<sup>1</sup>Arshid Mahmood Ali\*, <sup>2</sup>Aishah Mahpudiz, <sup>1</sup>Usman Saeed, <sup>1</sup>Sami U. Rather, <sup>1</sup>Ayyaz M. Nawaz  
<sup>1</sup>Javaid A and Hui Zhang

<sup>1</sup>Department of Chemical & Materials Engineering, King Abdulaziz University Jeddah,  
Kingdom of Saudi Arabia.

<sup>2</sup>Department of Chemical and Materials Engineering, University of Malaya, Malaysia.

<sup>3</sup>The Center of New Energy Materials and Technology, College of Chemistry and Chemical Engineering,  
Southwest Petroleum University, Chengdu 610500, China.  
amsali@kau.edu.sa\*

(Received on 26th November 2019, accepted in revised form 20th May 2020)

**Summary:** The aim of this study is to investigate the impact of an anionic precursor [N<sub>2</sub> gas and triethyleneamine (TEA) as nitrogen dopant source] to prepare anionic doped ZnO thin films surface morphologies, via a novel route - hydrothermal solution deposition at low temperature. The effect of dopant concentration under both with and without pH control was studied. The less populated doped ZnO crystal nearly had the same band gap as compared to undoped ZnO thin films. The photocatalytic activity of selected doped ZnO thin films were studied for the degradation of 10 mg L<sup>-1</sup> Methylene Blue under UV irradiation of 254nm. Based on the 1<sup>st</sup> order reaction rate constant results the morphology N2:S2-MS has shown highest degradation followed by N:S1-MS. Overall, the photocatalytic activity order is N2:S2-MS > N:S1-MS > N:S2-CG > N:S1-CG. In general, a significant variation in surface morphologies, crystal size and population, porosity and orientation were observed. This tailored-made variation enabled the doped ZnO thin films to successfully degrade the waste methylene blue effluents.

**Keywords:** Anionic doped zinc oxide thin film, Surface morphology, Crystal lattice, Degradation, Photocatalysis.

### Introduction

Zinc oxide (ZnO) has been used in a variety of form to demonstrate its diverse and multifunctional ability encompassed from wide range of application such as Photocatalyst [1-6], photoluminescence [7], optical activity properties [8] because of its high photosensitivity, wide band gap has a wide band gap [9-12], abundance availability, nontoxic and low cost [13, 14]. Suspended photocatalysts typically show a higher photocatalytic activity compared to supported catalysts because of an efficient mass transfer and better reactor design. The major disadvantage, however, is that suspended catalytic systems are extremely complicated to engineer since it is often difficult and expensive to separate the powdered catalyst from the product and/or waste streams. If this is not done, the catalyst goes to waste, unnecessarily increasing the waste disposal quantity and expense. Consequently, the recovery of the powdered catalyst usually did not remain economically viable [15, 16]. On the other hand, supported photocatalysts have had few issues of recovery at the end of the photocatalytic reaction, so long as the photocatalytic material remains intact and active throughout its lifetime (making lifetime mechanical strength and integrity, and photocatalytic activity with reuse two of the most important factors

in evaluating supported/immobilised photocatalysts). In author's previous studies [1, 3, 17] it was found that supported photocatalyst did not remain re-usable and stable depending upon the morphology. Surface defects, caused by Mars van Krevelen type reaction mechanism as concluded by [1] is some of the main reasons for this slackness. Therefore, the main objective of this study is to prepare and compare anionic doped nanostructured ZnO thin films with the undoped ZnO thin films and to study the impact of dopant on surface morphology and photocatalytically induced surface defects. Overall, the effect of the extent of dopant (both dopant precursor type and its concentration) on structure, morphology, band gap, crystallinity and pH of the reaction mixture used to obtain anionic doped ZnO thin films is discussed in detail.

### Experimental

#### Materials

The following chemicals were obtained from Sigma Aldrich: zinc nitrate hexahydrate (Zn(NO<sub>3</sub>)<sub>2</sub>·6H<sub>2</sub>O) 98%, polyethyleneimine (PEI) 50wt % solution in de-ionised water, nitrogen (N<sub>2(g)</sub>),

---

\*To whom all correspondence should be addressed.

triethylamine (TEA) 98.5%, 10% diluted ammonia solution (69%), 4% diluted nitric acid (70% purity), hexamethylenetetramine (HMT) synthesis grade and microscope glass slides (7105 WT). Deionised water (Millipore Milli Q A10) was used in all work.

### Methods

#### Preparation of Nitrogen-Doped Nano Structure Zinc Oxide Thin Films (N:ZnO).

Nitrogen-doped nanostructure ZnO (N:ZnO) thin films were prepared using two different dopant sources: N<sub>2</sub> gas and TEA.

#### N:ZnO thin films preparation using dopant N<sub>2</sub> gas

Freshly prepared nitrogen-saturated solutions of the reactants Zn(NO<sub>3</sub>)<sub>2</sub>·6H<sub>2</sub>O and HMT, each having a molar composition of 0.025 mol L<sup>-1</sup>, were mixed in a sealable glass jar containing a vertically suspended glass substrate (either clean glass slides -henceforth referred to as 'clean glass film growth' or CG or glass slides with an under-

layer of magnetron sputtered ZnO prepared via method as described by Ali *et al* [1, 6] - henceforth referred to as 'magnetron sputtered template growth or MS; with an approximate substrate top surface area of 2×1 cm<sup>2</sup>) on a custom-made Teflon support under an extensive supply of N<sub>2</sub> gas (to keep the N<sub>2</sub> saturation intact) using an N<sub>2</sub> gas sparger as shown in Fig. 1. The pH of the solutions was adjusted to a value of 5 or 7.5 by using diluted nitric acid (15%) or diluted ammonium hydroxide solution (28%). The sealed jar was then put into an oven at 95°C for 4 hours, after which the glass substrates were withdrawn from the solution, rinsed with deionised water and dried at 100°C [18] in the oven. The summary of this shown in Table 1. The films obtained from the new solution N:S1 [Zn(NO<sub>3</sub>)<sub>2</sub>·6H<sub>2</sub>O + HMT+ (saturated with N<sub>2</sub> gas) and pH 5 on magnetron sputtered template growth and clean glass substrate] were called N:S1-MS and N:S1-CG. Similarly, the films obtained from the new solution N:S2 [Zn(NO<sub>3</sub>)<sub>2</sub>·6H<sub>2</sub>O + HMT + PEI+ (saturated with N<sub>2</sub> gas) and pH 7.5 on magnetron sputtered template growth and clean glass substrate] were called N:S2-MS and N:S2-CG respectively.

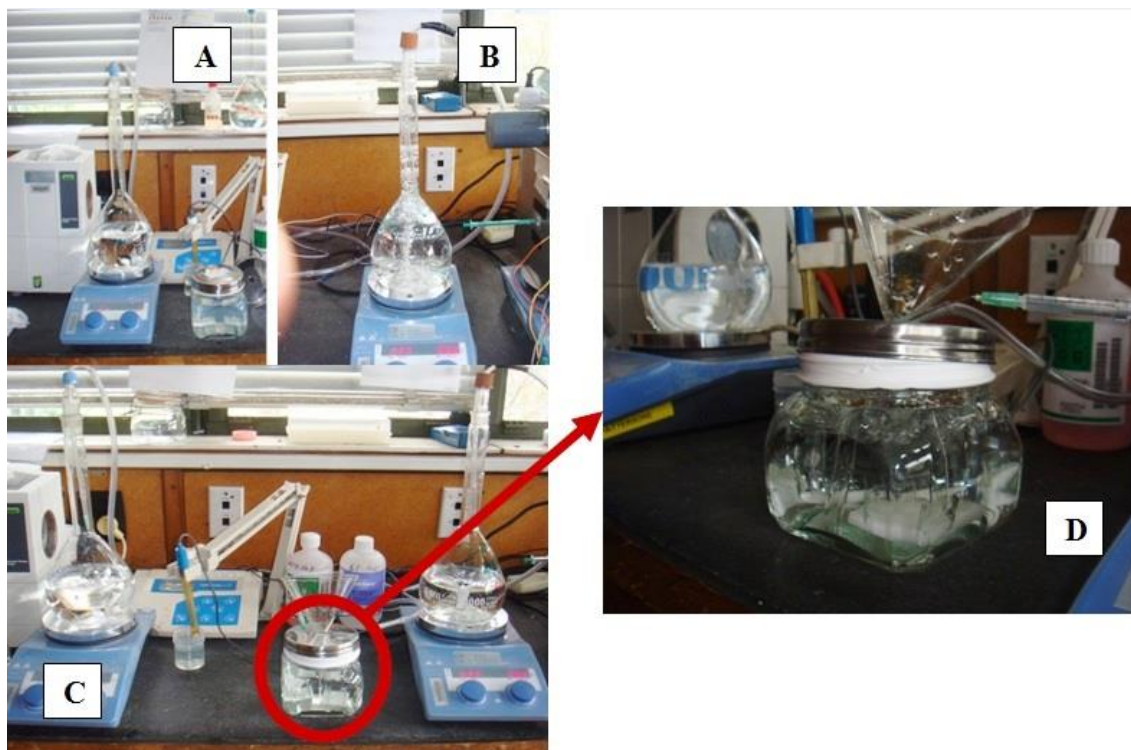


Fig. 1: Preparation of N:ZnO by using N<sub>2</sub> gas as nitrogen dopant source: (A) N<sub>2</sub> saturated Zn(NO<sub>3</sub>)<sub>2</sub>·6H<sub>2</sub>O; (B) N<sub>2</sub> saturated HMT; (C) Mixing of N<sub>2</sub> saturated Zn(NO<sub>3</sub>)<sub>2</sub>·6H<sub>2</sub>O and HMT under extensive supply of N<sub>2</sub>; (D) Magnified view of sealable glass jar

Table-1: Nitrogen-doped nanostructure ZnO thin films (N:ZnO) preparation conditions by using N<sub>2</sub> gas as nitrogen dopant source.

	N:S1-MS	N:S1-CG	N:S2-MS	N:S2-CG
pH	5	5	7.5	7.5
Solution composition	Zn(NO <sub>3</sub> ) <sub>2</sub> + HMT + N <sub>2</sub> gas	Zn(NO <sub>3</sub> ) <sub>2</sub> + HMT + N <sub>2</sub> gas	Zn(NO <sub>3</sub> ) <sub>2</sub> + HMT + PEI + N <sub>2</sub> gas	Zn(NO <sub>3</sub> ) <sub>2</sub> + HMT + PEI + N <sub>2</sub> gas

Table-2: Nitrogen doped nanostructured ZnO thin film (N:ZnO) preparation conditions by using TEA as Nitrogen dopant source.

Source of N <sub>2</sub> : Triethylamine (TEA)				
		Composition of Reaction Mixture	Substrate	Morphology
<b>Batch 1:</b>				
SA: 0.025 mol L <sup>-1</sup> TEA	37.5%	N':S1 = SA:SB:SC = 1.2:1:1	Template: MS and CG	N1:S1-MS N1:S1-CG
SB: 0.025 mol L <sup>-1</sup> Zn(NO <sub>3</sub> ) <sub>2</sub> .6H <sub>2</sub> O	31.5%	15% HNO <sub>3</sub> to maintain pH 5.0		
SC: 0.025 mol L <sup>-1</sup> HMT	31.5%			
pH = 5				
<b>Batch 2:</b>				
SA: 0.025 mol L <sup>-1</sup> TEA	37.5%	N':S2 = SA:SB:SC = 1.2:1:1	Template: MS	N2:S2-MS
SB: 0.025 mol L <sup>-1</sup> Zn(NO <sub>3</sub> ) <sub>2</sub> .6H <sub>2</sub> O	31.5%	0.3mL PEI		
SC: 0.025 mol L <sup>-1</sup> HMT	31.5%	28% NaOH to maintain pH 7.5		
pH = 7.5				
<b>Batch 3:</b>				
SA: 0.025 mol L <sup>-1</sup> TEA	16.67%	N'':S1 = SA:SB:SC = 0.4:1:1	Template: MS	N3:S1-MS
SB: 0.025 mol L <sup>-1</sup> Zn(NO <sub>3</sub> ) <sub>2</sub> .6H <sub>2</sub> O	41.67%	15% HNO <sub>3</sub> to maintain pH 5.0		
SC: 0.025 mol L <sup>-1</sup> HMT	41.67%			
pH = 5				
<b>Batch 4:</b>				
SA: 0.025 mol L <sup>-1</sup> TEA	16.67%	N'':S2 = SA:SB:SC = 0.4:1:1	Template: MS and CG	N4:S2-MS N4:S2-CG
SB: 0.025 mol L <sup>-1</sup> Zn(NO <sub>3</sub> ) <sub>2</sub> .6H <sub>2</sub> O	41.67%	0.3mL PEI		
SC: 0.025 mol L <sup>-1</sup> HMT	41.67%	28% NaOH to maintain pH 7.5		
pH = 7.5				
<b>Batch 5:</b>				
SA: 0.025 mol L <sup>-1</sup> TEA	37.5%	N''':S2 = SA:SB:SC = 1.2:1:1	Template: MS and CG	N5:S2-MS N5:S2-CG
SB: 0.025 mol L <sup>-1</sup> Zn(NO <sub>3</sub> ) <sub>2</sub> .6H <sub>2</sub> O	31.5%	0.3mL PEI		
SC: 0.025 mol L <sup>-1</sup> HMT	31.5%			
Without pH Control				
<b>Batch 6:</b>				
SA: 0.025 mol L <sup>-1</sup> TEA	16.67%	N''':S2 = SA:SB:SC = 0.4:1:1	Template: MS	N6:S2-MS
SB: 0.025 mol L <sup>-1</sup> Zn(NO <sub>3</sub> ) <sub>2</sub> .6H <sub>2</sub> O	41.67%	0.3mL PEI		
SC: 0.025 mol L <sup>-1</sup> HMT	41.67%			
Without pH Control				

### N:ZnO thin films preparation using TEA as nitrogen source

Table-2 summarised the six batches of N:ZnO thin films obtained by using TEA as a nitrogen source. Freshly prepared stock solutions of SA (TEA), (SB) Zn(NO<sub>3</sub>)<sub>2</sub>.6H<sub>2</sub>O and SC (HMT), each 0.025molL<sup>-1</sup>, were mixed in either ratio 1.2:1:1 or 0.4:1:1, in a sealable glass jar containing vertically suspended glass substrate (CG and MS) on a custom-made Teflon support. The pH of the solutions was adjusted to a value of 5 or 7.5 by using diluted nitric acid (15%) or diluted ammonium hydroxide solution (28%). The sealed jar was then put into an oven at 95°C for 4 hours, after which the glass substrates were withdrawn from the solution, rinsed, wiped on the underside with deionised water, and dried at room temperature. The films obtained from different batches 1-2 (Table 2) on magnetron sputtered template growth were called N1:S2-MS, N2:S2-MS respectively; batches 3-4 (Table 2) on magnetron sputtered template growth and clean glass slides were called N3:S2-MS, N4:S2-MS, N3:S2-CG and N4:S2-CG respectively;

batch 5 (Table 2) on magnetron sputtered template growth, and clean glass slides, were called N5:S1-MS and N5:S1-CG respectively; and those from batch 6 (Table 2) on magnetron sputtered template growth were called N6:S1-MS.

### Characterisation of ZnO films

The surface and cross-sectional morphologies of ZnO thin films (both undoped and doped) were characterised by scanning electron microscopy (SEM) using a Philips XL-30s operating at 5kV. This characterisation involved measuring the thin film thickness, the effect of reaction on morphology, and attrition/stress on the surface caused by UV irradiation. Both top surface and cross-sections were imaged. Cross-sectioning was carried out by cutting the thin film sample into two parts using wire cutters whilst holding it with pliers. Polaron SC 7640 Sputter Coater was used to give a very thin, minimal Pt coating (600 seconds) suitable for SEM viewing. The crystallinity and the phases present in both undoped and doped nanostructure

ZnO thin films were characterised by using an X-ray diffractometer (XRD) with Cu-K $\alpha$  radiation (Bruker D8). Undoped and doped nanostructure ZnO thin films were glued horizontally to the base of the sample holder in such a way that the top surface of ZnO thin films faced upward. Angle of incident ( $2\theta$ ) range were adjusted to 30-65 and 30-70 for undoped and doped ZnO thin films respectively. Bruker AXS: EVA software was used to study the change in crystallinity and number of phases before and after reaction.

## Results and Discussions

### Impact of Dopant on Surface Morphologies

The nature and type of morphology, summarised in author's previous studies [1, 6], also as shown in Fig. 2, plays an important role in photocatalytic activity and reaction mechanism. Therefore and in order to preserve this parameter, anionic dopant (nitrogen) [19-23] were used to obtain a morphology as close as possible to undoped ZnO thin films. Dopant usually reduces the band gap (hence metal oxide is expected to be more active at low UV energy or at higher UV irradiation wavelength) [24] and the delocalisation of the d-states in the band gap of metal oxide, which helps in reducing the recombination chances of UV-induced electron-hole pairs [25]. The extent of dopant, both type and concentration, on both surface morphology and band gap, is summarised in the following sections.

### Nitrogen-doped Zinc Oxide (N:ZnO) Nanostructured Thin Films

The effect of each source of nitrogen (nitrogen gas (N<sub>2</sub>) and Triethylamine (TEA) on surface morphology, crystallinity, band gap and associated surface defects along with the lack or presence of nitrogen incorporation, are summarised in the following sections.

### N:ZnO thin film morphologies obtained by using N<sub>2</sub> gas as nitrogen source

A top surface view of the SEM image of the nitrogen-doped morphology, obtained from the mixture of solutions (N:S1) on a magnetron sputtered coated ZnO glass template, (N1:S1-MS) is shown in Fig. 3A. The morphology (N:S1-MS) was nearly same as undoped S1-MS. No significant differences in crystal structure, size and smoothness were noticed except in the population and the orientation of crystals. However, no clear indication of N<sub>2</sub> incorporation was depicted by EDX analysis (Fig.3B). Most of the crystals are positioned at a greater inclination than that for undoped nanostructured ZnO thin films (Fig. 2A). The band gap was approximately the same as for the undoped: another indication of inefficient dopant incorporation in the ZnO crystal

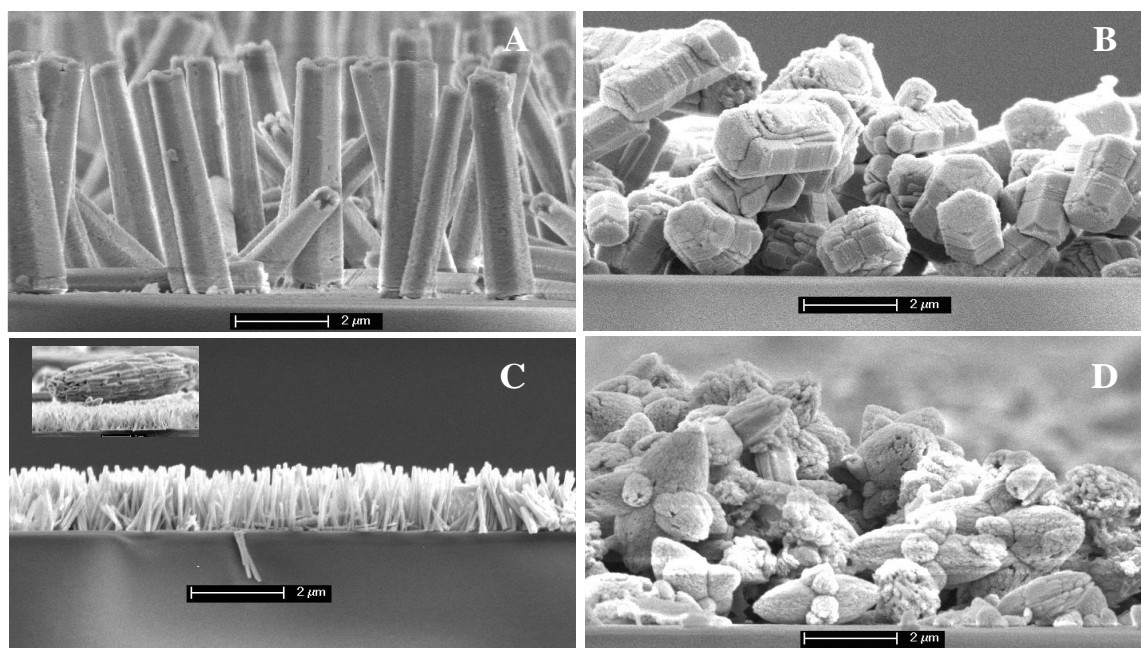


Fig. 2: Undoped ZnO thin films surface morphologies obtained in author's previous studies [6].

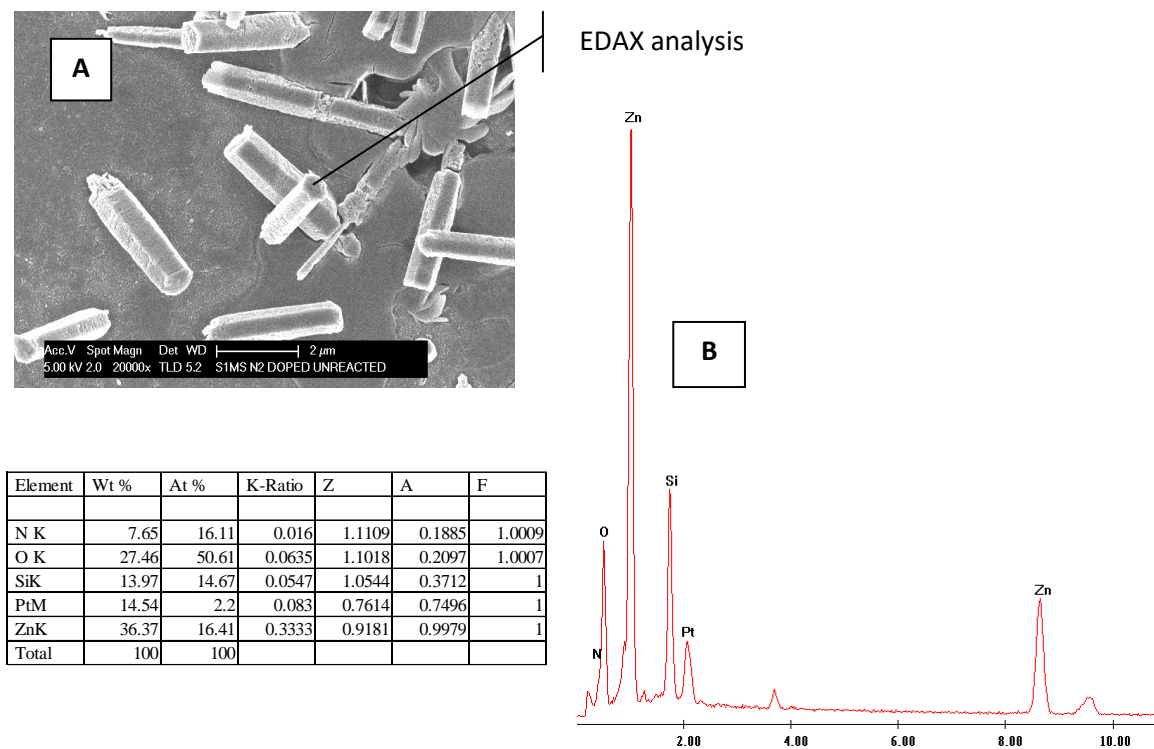


Fig. 3: (A): SEM image (top view) of nitrogen-doped nanostructured ZnO thin films N1:S1-MS; (B) :EDX analysis at position P1(ZnO single crystal).

Morphology (N:S1-CG; Fig. 4A), obtained on a clean glass slide from a mixture of solutions (N:S1), shows a clear difference in the surface morphology, compared to undoped nanostructured ZnO thin films (Fig. 2B). Both crystal structure and smoothness were severely affected. EDX analysis (Fig. 4B) did not show any solid evidence of the presence, (and hence the incorporation) of nitrogen that might be due to the lack of interaction of nitrogen source species with ZnO, in the ZnO crystal.

Morphologies obtained from a mixture of solutions N:S2, on MS and CG substrate, are shown in Figs. 5-6; morphology N:S2-MS showed a significant variation in the surface structure (Fig. 5A) compared to undoped S2-MS (Fig. 2C). A huge proportion of large crystal similar to undoped S2-CG was seen on the top of the MS layer with little growth and reduced porosity. Morphology N:S2-CG (Fig. 6) was almost similar to undoped nanostructured ZnO thin films S2-CG. No evidence of N<sub>2</sub> incorporation into morphologies N:S2-MS and N:S2-CG, similar to N:S1-MS and N:S1-CG, was noticed (Fig. 5B and Fig. 6B).

The doped morphologies (N:ZnO), obtained by using N<sub>2</sub> gas as a nitrogen dopant source, were

affected not only in terms of surface morphologies; as well as EDX analysis did not show any solid evidence of the presence of nitrogen in the ZnO lattice or lattice interstices and these cannot therefore be considered to be as nitrogen doped morphologies, although the presence nitrogen gas (nitrogen saturated mixture of solutions N:S1 and N:S2) had imparted a significant effect on surface morphologies. In general, the bubbling/mixing of nitrogen gas technique, to achieve a nitrogen saturated reaction mixture, is not an efficient way to enable nitrogen to produce N:ZnO thin films. Therefore, another soluble source of nitrogen, such as TEA, was attempted to obtain N:ZnO nanostructured thin films.

#### *N:ZnO thin films morphologies obtained by using TEA as an N<sub>2</sub> source*

Six attempts were made to prepare N:ZnO thin films by using TEA as a nitrogen dopant source at two different concentrations (high and low concentrations of TEA; 37% or 16.7% respectively) with and without pH control. The effect of TEA as a nitrogen source on surface morphology is summarised in the following sections.

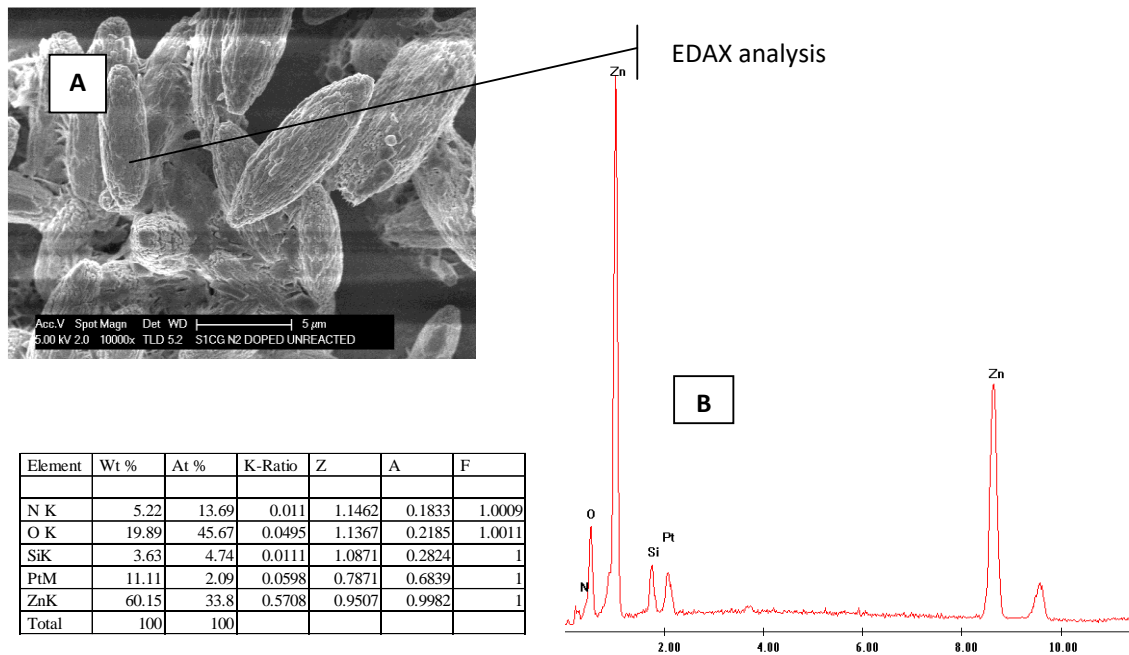


Fig. 4: A: SEM image (top view) of N:S1-CG; B:EDX analysis at position P1(ZnO single crystal).

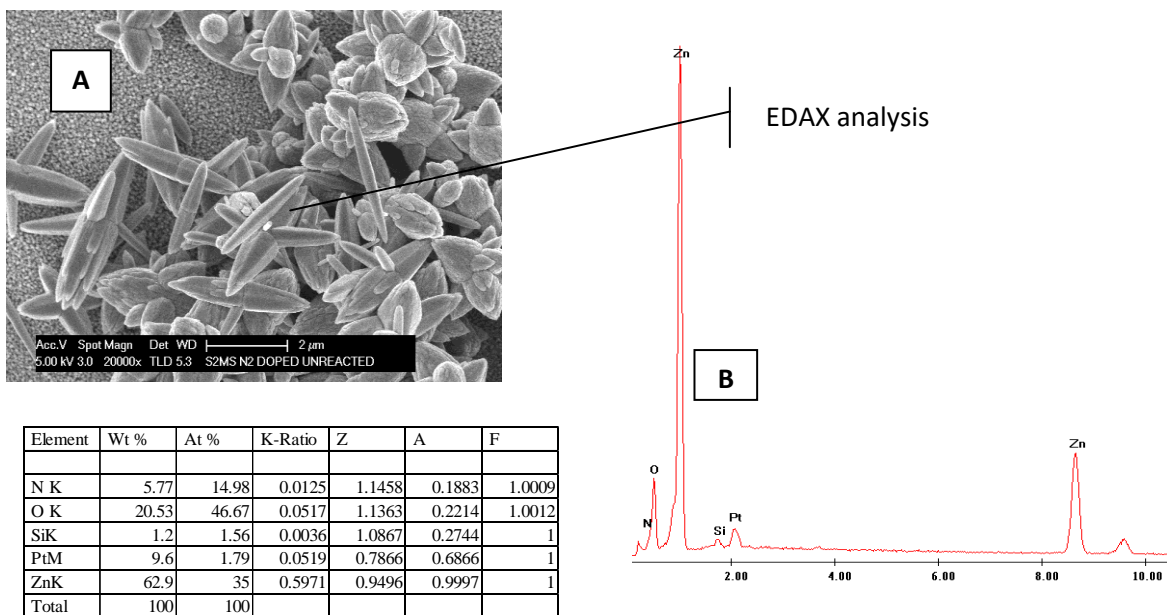


Fig. 5: A: SEM image (top view) of N:S2-MS; B: EDX analysis at position P1(complex ZnO single crystal).

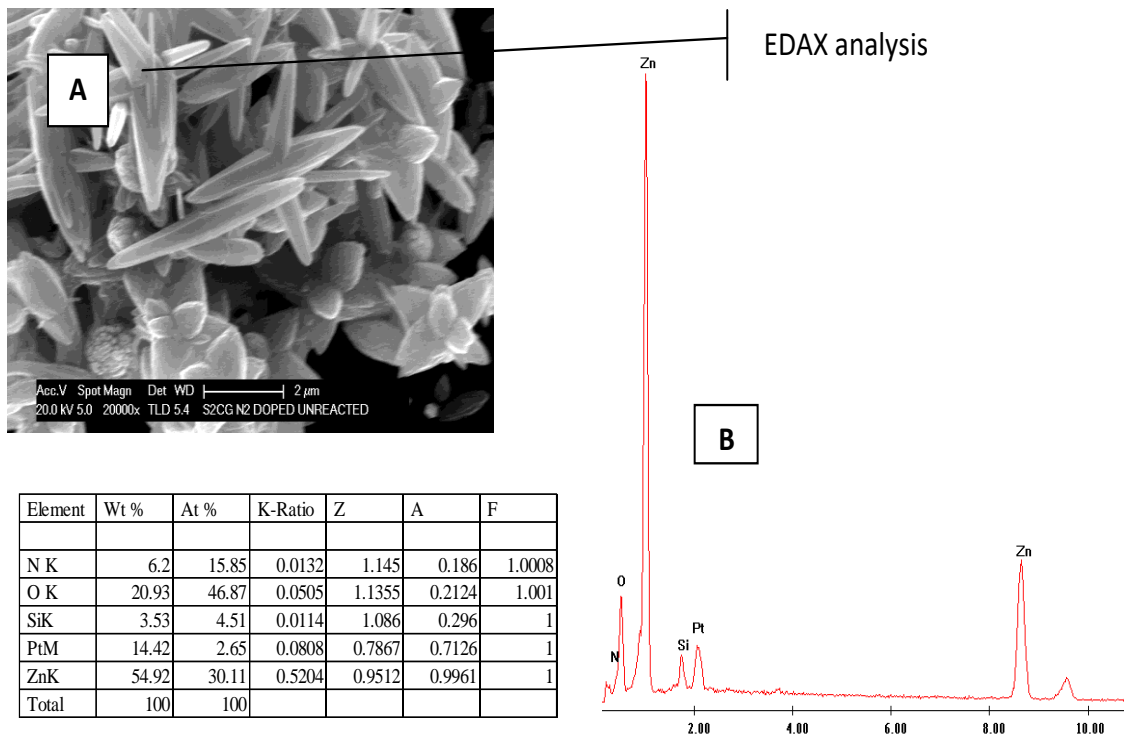


Fig.6: A: SEM image (top view) of N:S2-CG; B: EDX analysis at position P1 (complex ZnO single crystal).

#### Morphologies obtained at high concentration of TEA with pH control

Figs. 7-9 shows three different morphologies, N1:S1-MS, N1:S1-CG and N2:S2-MS, obtained from a high concentration of TEA (37.5%), on MS or CG glass substrate by using two different mixtures of solutions N':S1 and N':S2, with pH control 5 or 7.5. N:ZnO morphologies obtained by using TEA as an N<sub>2</sub> dopant source also showed huge variations in morphologies compared to undoped ZnO thin films (see Fig.2). Morphology N1:S1-MS (Fig. 7A) obtained, at pH 5, had both solid and X-shaped, and horizontally aligned, hollow crystal structures. Again, no solid evidence of nitrogen incorporation as dopant was found (see Fig. 7B: EDX analysis at position P1 (X-shaped hollow crystal) and Fig. 7C: EDX analysis at position P2 (crystal growth near to MS layer).

Morphology N1:S1-CG (Fig. 8A) obtained on the CG substrate from the reaction mixture of solution N':S1, at pH 5, had also shown a significant

variation in crystal orientation, size and population, compared to undoped S1-CG thin films (see Fig. 2B). Although the presence of TEA left a huge impact on surface morphologies, no evidence of the presence of nitrogen was revealed by EDX analysis (Figs. 8B-C) at the two different positions on surface P1 and P2

The top surface and cross-sectional views of the morphology N2:S2-MS (Figs. 9A and 10A), obtained on MS substrate by using solution N':S2 at pH 7.5, differ greatly in crystal structure, crystal smoothness, crystal size and orientation compared to undoped S2-MS (see Fig. 2C) obtained under similar conditions, except for the presence of TEA. Horizontally oriented cusps of ZnO were seen that could be caused by the interaction of TEA with other reacting species like Zn(NO<sub>3</sub>)<sub>3</sub>·6H<sub>2</sub>O, HMT and PEI. No evidence of the incorporation of nitrogen as a doped element was noticed, similar to N1:S1-MS and N1:S1-CG, as shown by EDX analysis (Figs 9B-C and 10B-C).

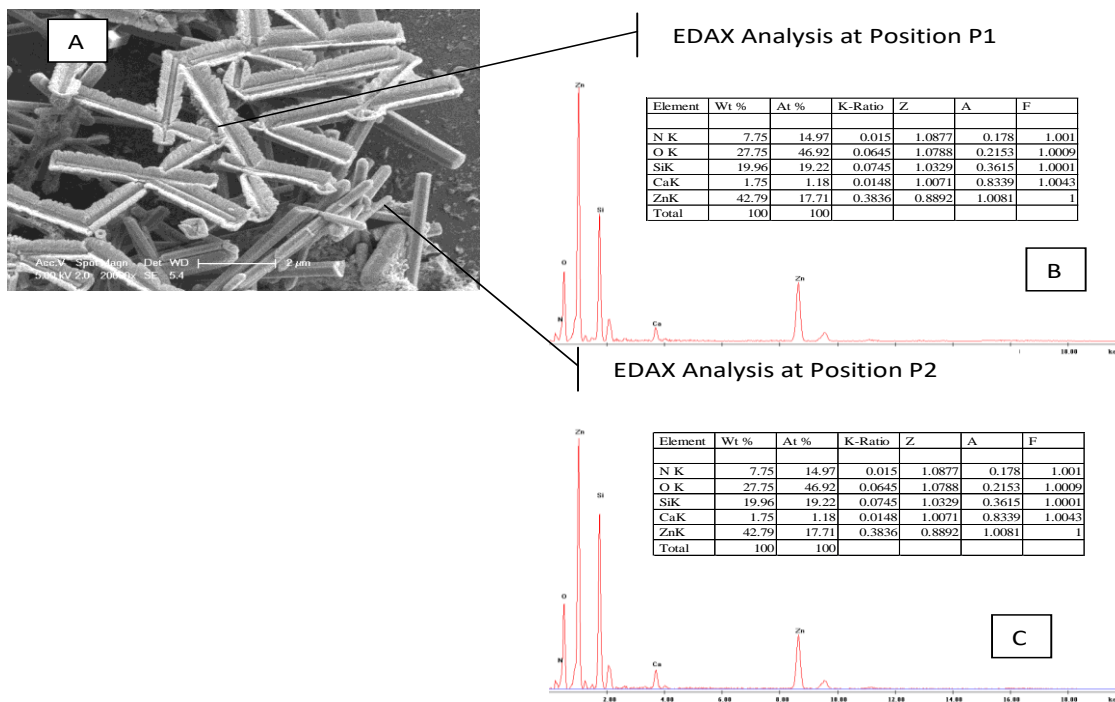


Fig.7: A: SEM image (top view) of N1:S1-MS; B: EDX analysis at position P1 (X-shaped ZnO crystal); C: EDX analysis at position P2 (layer upon magnetron sputtered coating and small ZnO crystal) at high concentration of TEA with pH control.

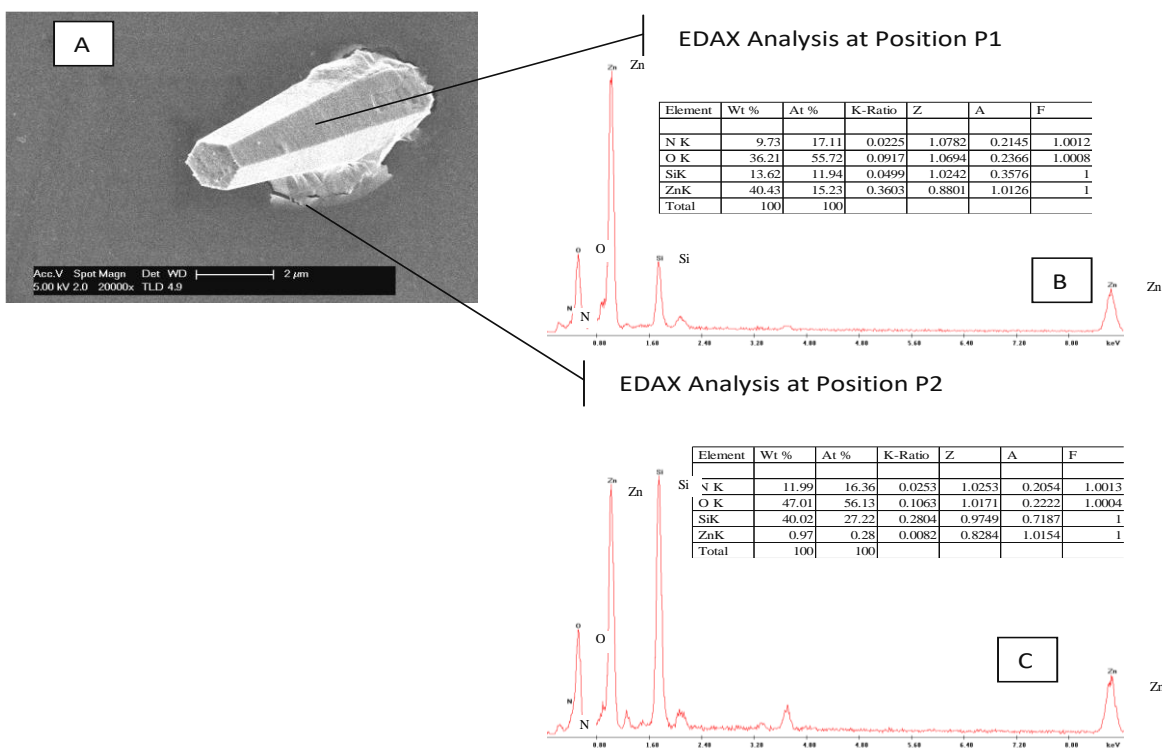


Fig. 8: (A): SEM image (top view) of N1:S1-CG; B:EDX analysis at position P1(regular ZnO crystal); C:EDX analysis at position P2(layer upon magnetron sputtered coating ) at high concentration of TEA with pH control.

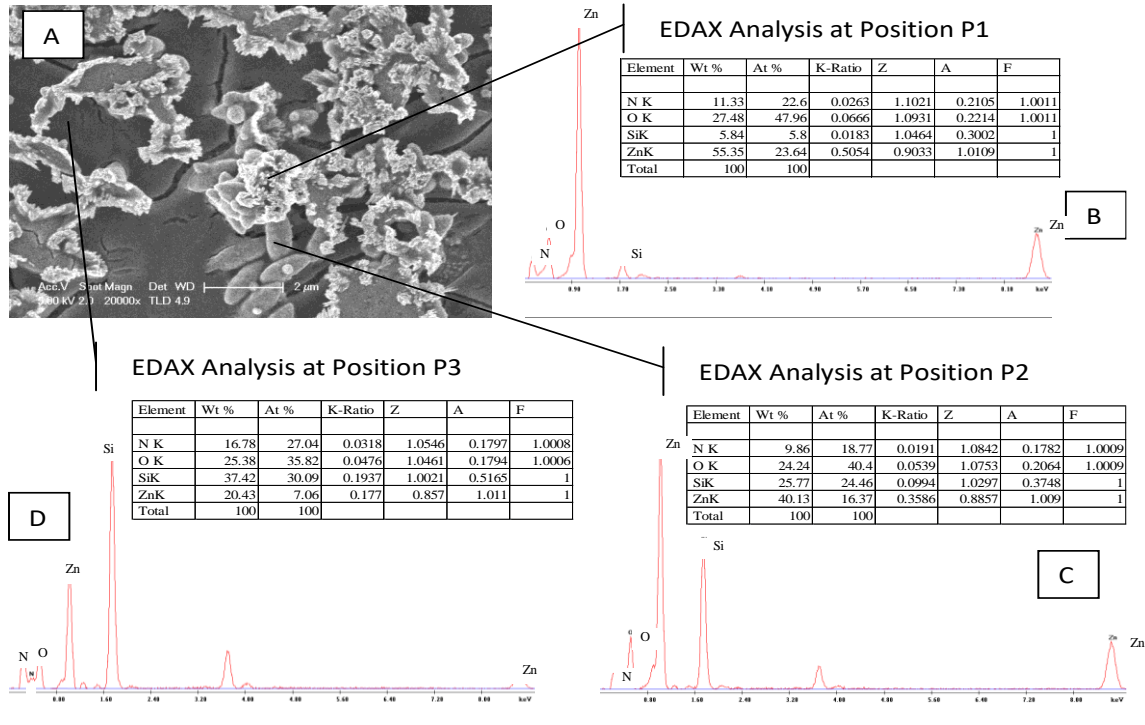


Fig. 9: A: SEM image (top view) of N2:S2-MS; B: EDX analysis at position P1(cluster of ZnO crystal); C: EDX analysis at position P2(ZnO single crystal); D: EDX analysis of at position P3 (layer upon magnetron sputtered coating).

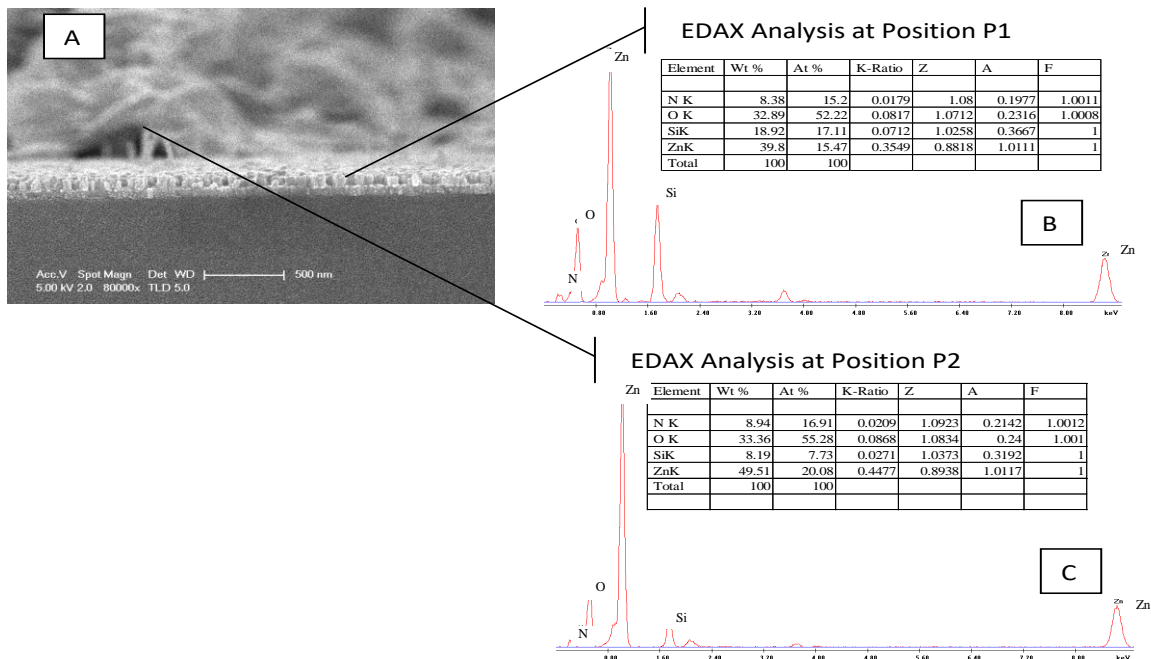


Fig. 10: A: SEM image (cross-sectional) of N2:S2-MS; B: EDX analysis at position P1 (cluster of ZnO crystal); C: EDX analysis at position P2(complex ZnO single crystal).

*Morphologies obtained at low concentration of TEA with pH control*

A marked variation in surface morphologies of N:ZnO thin films could be a result of higher concentration of the TEA. In order to investigate and to optimise nitrogen incorporation [26] as a dopant as well as the concentration of TEA, and to have lower impact of dopant on surface morphologies, a lower concentration of TEA (16.7%) was used. Figs. 11-13 show the morphologies obtained at low TEA concentration with pH 5 or 7.5. Little effect of the

TEA concentration was noticed. Nearly similar patterns of morphologies N4:S2-MS (Fig. 11A) and N4:S2-CG (Fig. 12A) i.e. complex, hollow and fragile crystals, was obtained at a lower concentration of TEA, except for morphology N3:S1-MS (Fig. 10A), which had shown a lower level of crystal population and incomplete growth of crystals. Little presence of nitrogen incorporation in the crystal lattice could be measured (see Figs. 10B-C, 11B-C and Figs. 12B-C; EDX analysis at two different position P1: crystal surface and P2: layer on MS or CG substrate).

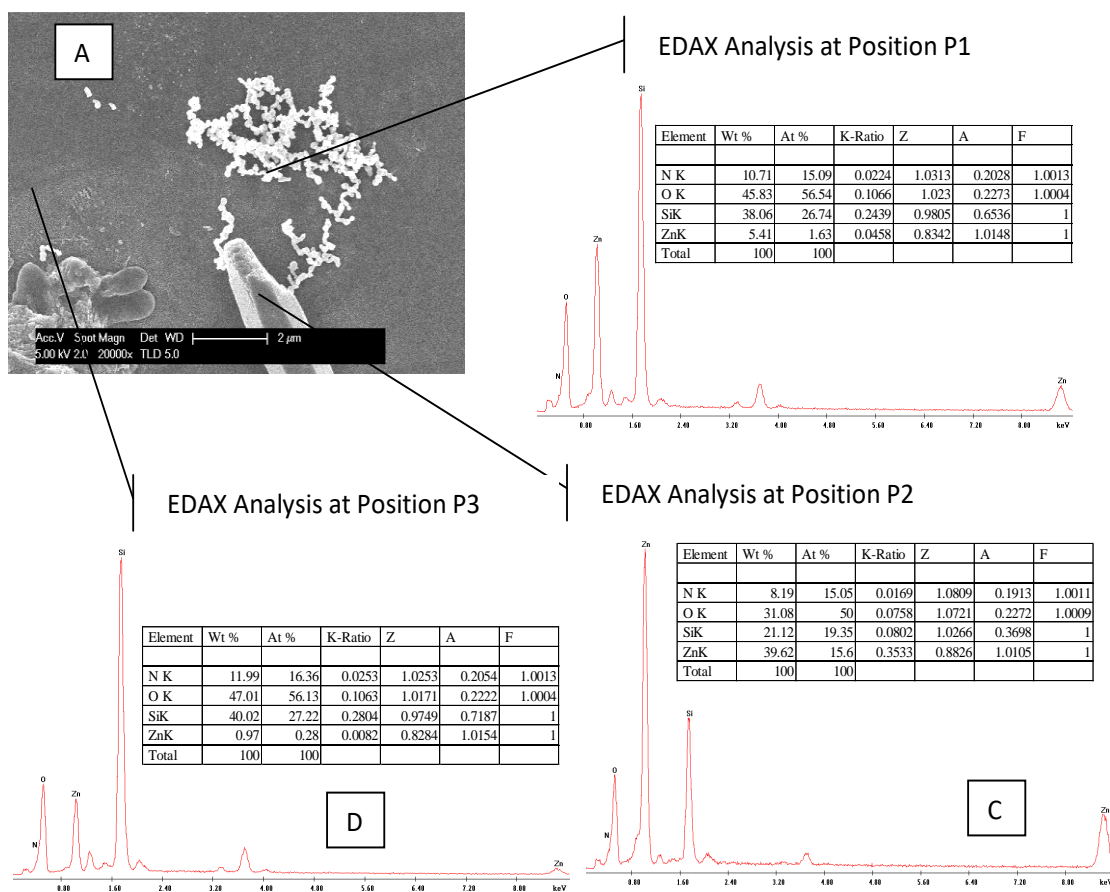


Fig. 11: A: SEM image (top view) of N3:S1-MS; B: EDX analysis at position P1 (cluster of small ZnO crystals); C: EDX analysis at position P2 (large ZnO crystal); D: EDX analysis at position (layer upon magnetron sputtered coating) at low concentration of TEA with pH control.

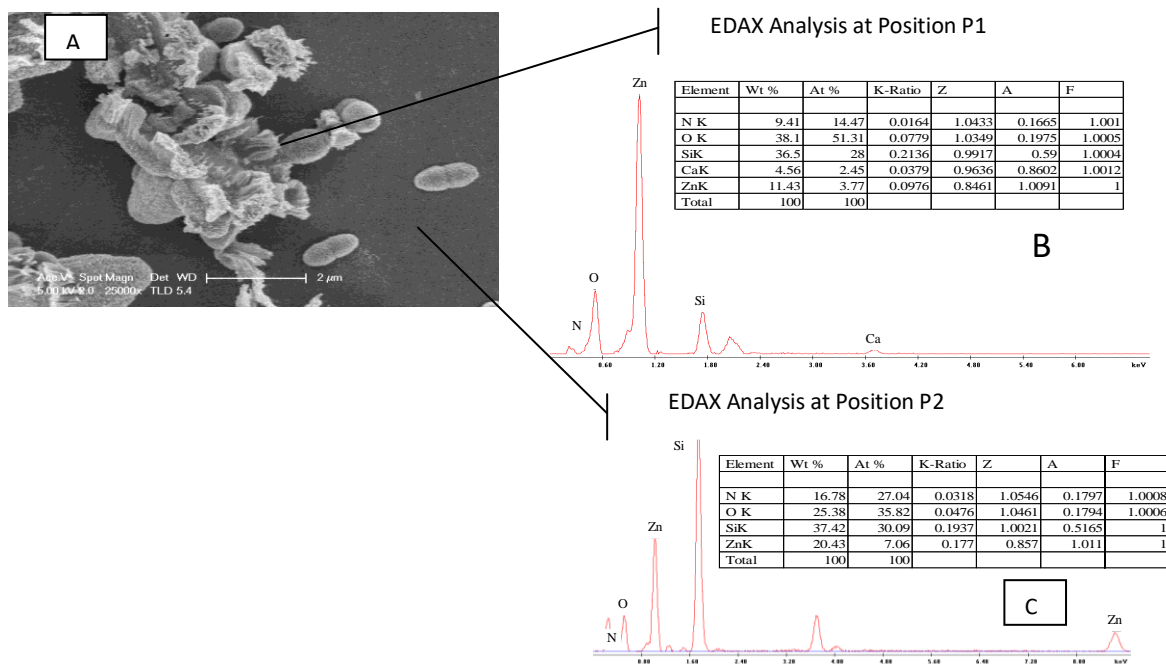


Fig. 12: A: SEM image (top view) of N4:S2-MS; B: EDX analysis at position P1(cluster of ZnO crystal); C: EDX analysis at position P2(layer upon magnetron sputtered coating).

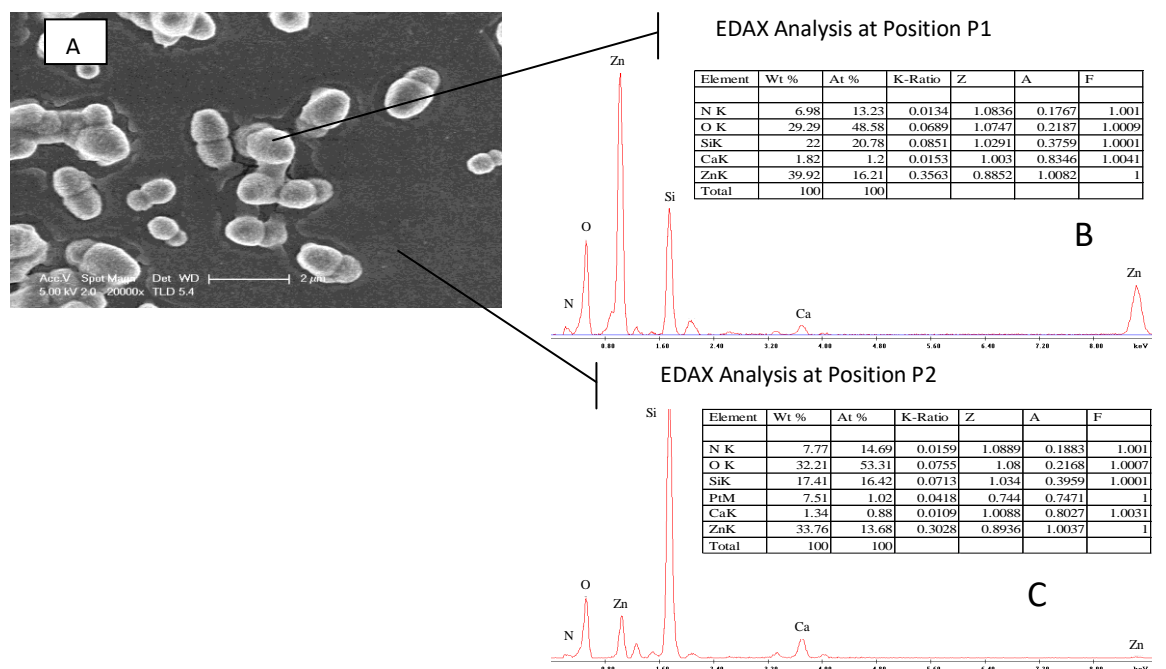


Fig. 13: A: SEM image (top view) of N4:S2-CG; B: EDX analysis at position P1(ZnO jointed crystal); C: EDX analysis at position P2 (layer upon magnetron sputtered coating) at low concentration of TEA with pH control.

### Morphologies obtained at high and low concentrations of TEA without pH control

A change in TEA concentration did not reveal any significant improvement in the nitrogen incorporation as dopant into the ZnO crystal lattice. The only other parameter that might control the surface morphology is the pH of the reaction mixture. To study and investigate the role of pH, a set of nitrogen-doped structures/morphologies (N5:S2-MS, N5:S2-CG and N6:S2-MS) were also prepared under both high and low concentration of TEA without maintaining pH (results obtained are shown in Figs. 14-16). A significant effect of pH was noticed on the crystals formed (fairly large compact structures), although none of the nitrogen-doped morphologies were suitable, from the point of view of either nitrogen incorporation (see Figs. 14B-C, 15B-C and 16B-C), or surface morphology, as shown in Figs. 14A, 15A and 16A.

### Photocatalytic Activity

To check the photocatalytic activity of doped zinc oxide thin films, four catalyst sample N:S1-MS, N:S1-CG, N2:S2-MS and N:S2-CG were opted among all prepared nitrogen doped zinc oxide thin films. The photocatalytic activity was measured for the degradation of 10 mg L<sup>-1</sup> Methylene Blue under UV irradiation of 254nm. The 1<sup>st</sup> order reaction rate constant results on

liquid volume basis ( $k_{app}$ : s<sup>-1</sup>), catalyst mass basis ( $k'_{app}$ : m<sup>3</sup>kg<sup>-1</sup>s<sup>-1</sup>) and a UV exposed surface area ( $S$ ) basis ( $k''_{app}$ : m<sup>3</sup> m<sup>-2</sup> s<sup>-1</sup>) four selected doped N:S1-MS, N:S1-CG, N2:S2-MS and N:S2-CG photocatalyst is shown in Table 1. Among all the selected sample, the morphology N2:S2-MS has shown highest degradation followed by N:S1-MS. In general, the photocatalytic activity order is N2:S2-MS > N:S1-MS > N:S2-CG > N:S1-CG. Based on available relevant literature under exact photocatalytic activity test conditions and N:ZnO thin films preparation method, no study is reported. For instance, Shinde *et al* [27] concluded that nitrogen doped zinc oxide thin films (prepared by chemical spray pyrolysis – a different method to the method reported in the submitted manuscript) showed higher Toulene degradation ability as to undoped ZnO thin films. The similar results as in our case, but we study degradation of Methylene blue by using N:ZnO thin film prepared by novel route – hydrothermal solution deposition. Similarly, Vasile *et al* [28] concluded that nitrogen doped zinc oxide thin films prepared by high power impulse magnetron sputtering has higher water splitting capability as to the undoped zinc oxide thin film. Therefore, we strongly believe that the opted catalysts preparation approach/technique is capable to tailor the morphology for a wide range of waste effluents treatment.

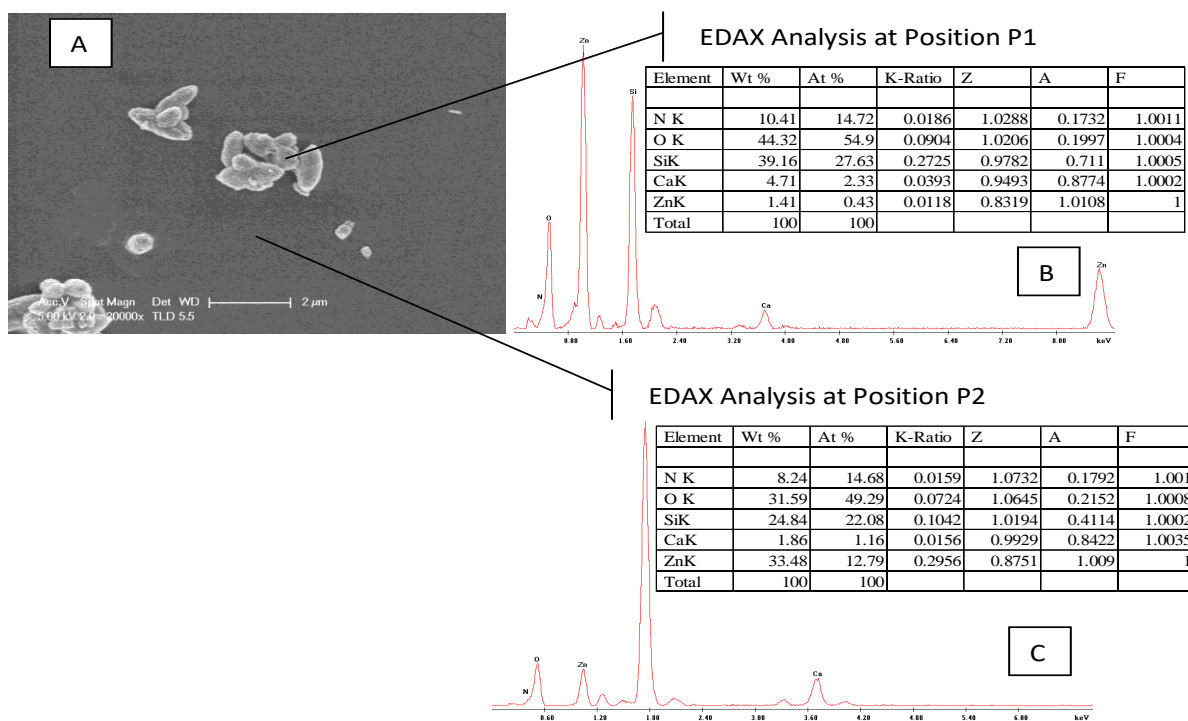


Fig. 14: A: SEM image (top view) of N5:S2-MS; B: EDX analysis at position P1(cluster of ZnO crystal); C:EDX analysis at position P2(layer upon magnetron sputtered coating) at high concentration of TEA without pH control.

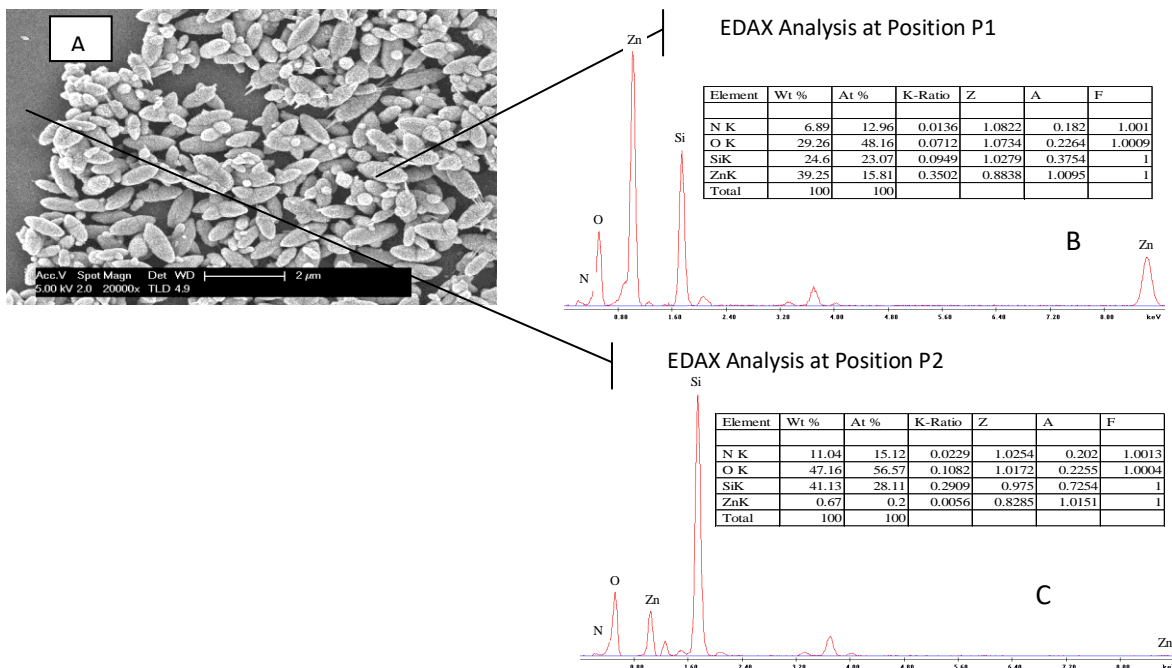


Fig. 15: A: SEM image (top view) of N5:S2-CG; B:EDX analysis at position P1(edged ZnO crystal); C:EDX analysis at position P2(layer upon magnetron sputtered coating) at high concentration of TEA without pH control.

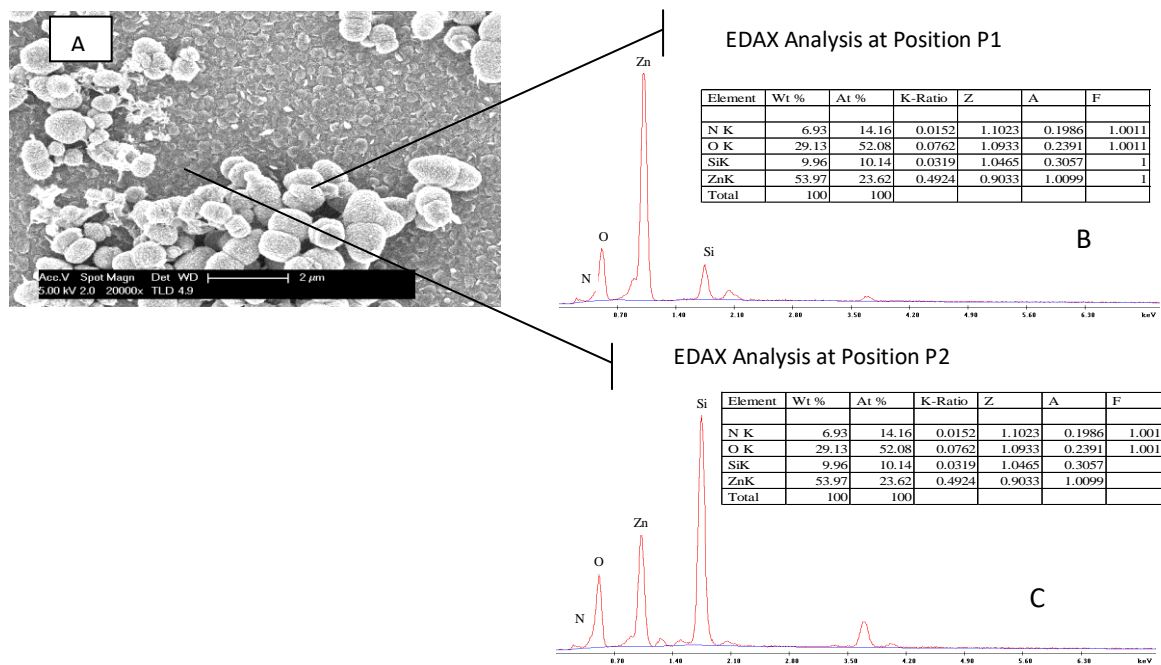


Fig. 16: A: SEM image (top view) of N6:S2-MS; B:EDX analysis at position P1(cluster of ZnO crystal); C:EDX analysis at position P2(flowery layer upon magnetron sputtered coating) at low concentration of TEA without pH control.

Table-3: Summary of 1<sup>st</sup> order reaction rate constant on liquid volume basis ( $k_{app}$ : s<sup>-1</sup>), catalyst mass basis ( $k'_{app}$ : m<sup>3</sup>kg<sup>-1</sup>s<sup>-1</sup>) and a UV exposed surface area ( $S$ ) basis ( $k''_{app}$ : m<sup>3</sup> m<sup>-2</sup> s<sup>-1</sup>) for the photocatalysed degradation of 10 mg L<sup>-1</sup> Methylene Blue under UV irradiation of 254nm.

Selected doped photocatalyst	Estimated UV exposed surface area $S$ (m <sup>2</sup> )	First order rate constants (UV irradiation of 254nm)		
		$k_{app}$ (s <sup>-1</sup> )	$k'_{app}$ (m <sup>3</sup> kg <sup>-1</sup> s <sup>-1</sup> )	$k''_{app}$ (m <sup>3</sup> m <sup>-2</sup> s <sup>-1</sup> )
N:S1-MS	3.79 ×10 <sup>-4</sup>	1.075 ×10 <sup>-2</sup>	1.018	0.56 ×10 <sup>-3</sup>
N:S1-CG	2.99 ×10 <sup>-4</sup>	2.295 ×10 <sup>-3</sup>	0.232	1.29 ×10 <sup>-4</sup>
N2:S2-MS	1.87 ×10 <sup>-3</sup>	2.935 ×10 <sup>-2</sup>	2.781	1.54 ×10 <sup>-3</sup>
N:S2-CG	3.85 ×10 <sup>-4</sup>	3.0 ×10 <sup>-3</sup>	0.284	1.58 ×10 <sup>-4</sup>

## Conclusions

The doped morphologies (N:ZnO), obtained by using N<sub>2</sub> gas and/or TEA as a nitrogen dopant source, were of varied nature in terms of crystal size, porosity and orientation. The EDX analysis showed the presence of nitrogen in the ZnO lattice or lattice interstices. In general, the bubbling/mixing of nitrogen gas and/or the stoichiometric ratio of TEA, is an efficient way to incorporate nitrogen to produce N:ZnO thin films. Both the concentration of each dopant and pH of the reaction mixture played significant roles in changing the surface morphologies, a clear indication that the presence of TEA in the reaction mixture has a marked effect on the affinity of various reaction species such as Zn(NO<sub>3</sub>).6H<sub>2</sub>O, HMT and/or PEI. The photocatalytic activity of selected doped ZnO thin films were also studied for the degradation of 10 mg L<sup>-1</sup> Methylene Blue under UV irradiation of 254nm. Based on the 1<sup>st</sup> order reaction rate constant results the morphology N2:S2-MS has shown highest degradation followed by N:S1-MS. Overall, the photocatalytic activity order is N2:S2-MS > N:S1-MS > N:S2-CG > N:S1-CG. Because of varied nature in surface morphologies, the use of TEA/N<sub>2</sub> gas as anionic dopant has a potential to acquire/achieved tailored-made surface morphologies for a wide range of industrial applications/processes.

## Acknowledgements

This project was funded by the Deanship of Scientific Research (DSR), King Abdulaziz University, Jeddah, under grant No. (DF-870-130-1441). The authors, therefore, gratefully acknowledge DSR technical and financial support.

## References

1. A. M. Ali, E. A. C. Emanuelsson, D. A. Patterson, Conventional versus lattice photocatalysed reactions: Implications of the lattice oxygen participation in the liquid phase photocatalytic oxidation with nanostructured ZnO thin films on reaction products and mechanism at both 254 nm and 340 nm, *Appl. Catal B: Env*, **106** 323 (2011).
2. U. I. Gaya, A. H. Abdullah, Z. Zainal, M. Z. Hussein, Photocatalytic treatment of 4-chlorophenol in aqueous ZnO suspensions: Intermediates, influence of dosage and inorganic anions, *J. Hazard. Mater*, **168** 57 (2009).
3. C. J. Mcfarlane, E. A. C. Emanuelsson, A. M. Ali, W. Gao, D. A. Patterson, Optimising Zinc Oxide Nanostructured Thin Films as Photocatalyst for Industrial Wastewaters, *Int. J. Chem. Eng.*, **2**, 63 (2010).
4. J. Yu, X. Yu, Hydrothermal synthesis and photocatalytic activity of zinc oxide hollow spheres, *Environ. Sci. Technol*, **42**, 4902 (2008).
5. R. P. K. Wells, Wiley-VCH Verlag GmbH & Co. KGaA, 2009, pp. 755.
6. A. M. Ali, E. A. C. Emanuelsson, D. A. Patterson, Photocatalysis with nanostructured zinc oxide thin films: The relationship between morphology and photocatalytic activity under oxygen limited and oxygen rich conditions and evidence for a Mars Van Krevelen mechanism, *Appl. Catal B: Env*, **97** 168 (2010).
7. A. Nakagawa, F. Masuoka, S. Chiba, H. Endo, K. Meguro, Y. Kashiwaba, T. Ojima, K. Aota, I. Niikura, Photoluminescence properties of nitrogen-doped ZnO films deposited on ZnO single crystal substrates by the plasma-assisted reactive evaporation method, *Appl. Surf. Sci.*, **254**, 164 (2007).
8. Q. Xu, S. Zhou, D. Marko, K. Potzger, J. Fassbender, M. Vinnichenko, M. Helm, H. Hochmuth, M. Lorenz, M. Grundmann, H. Schmidt, Paramagnetism in Co-doped ZnO films, *J. Phys. D Appl. Phys.*, **42**, (2009).
9. R. Kavitha, S. Meghani, V. Jayaram, Synthesis of titania films by combustion flame spray pyrolysis technique and its characterization for photocatalysis, *Mater. Sci.: B*, **139** 134 (2007).
10. N. Daneshvar, S. Aber, M. S. S. Dorraji, A. R. Khataee, M. H. Rasoulifard, Preparation and investigation of photocatalytic properties of ZnO nanocrystals: effect of operational parameters and kinetic study.(Report), *Int. J. Chem. and Biomol. Eng*, **1** 24 (2008).

11. O. A. Fouad, A. A. Ismail, Z. I. Zaki, R. M. Mohamed, Zinc oxide thin films prepared by thermal evaporation deposition and its photocatalytic activity, *Appl. Catal B: Env*, **62** 144 (2006).
12. S. Chakrabarti, B. K. Dutta, Dye-sensitized photocatalytic degradation of PVC-ZnO composite film, *Int J Environ Tech Manag*, **9**, 34 (2008).
13. A. Akyol, H. C. Yatmaz, M. Bayramoglu, Photocatalytic decolorization of Remazol Red RR in aqueous ZnO suspensions, *Applied Catalysis B: Environmental*, **54** 19 (2004).
14. M. J. Height, S. E. Pratsinis, O. Mekasuwandumrong, P. Praserttham, Ag-ZnO catalysts for UV-photodegradation of methylene blue, *Appl. Catal B: Env*, **63** 305 (2006).
15. K. Kabra, R. Chaudhary, R. L. Sawhney, Treatment of hazardous organic and inorganic compounds through aqueous-phase photocatalysis: A review, *Ind. Eng. Chem. Res.*, **43** 7683 (2004).
16. J. V. Anderson, H. Link, M. Bohn, B. Gupta, *Sol. Energy Mater.*, **24** 538 (1991).
17. A. M. Ali, E. A. C. Emanuelsson, D. A. Patterson, Photocatalysis with nanostructured zinc oxide thin films: The relationship between morphology and photocatalytic activity under oxygen limited and oxygen rich conditions and evidence for a Mars Van Krevelen mechanism, *Appl. Catal B: Env*, **97** 168 (2009).
18. A. Wang, B. Zhang, X. Wang, N. Yao, Z. Gao, Y. Ma, L. Zhang, H. Ma, Nano-structure, magnetic and optical properties of Co-doped ZnO films prepared by a wet chemical method, *J Phys. D Appl. Phys.*, **41** (2008).
19. E. Borgarello, J. Kiwi, M. Graetzel, E. Pelizzetti, M. Visca, Visible light induced water cleavage in colloidal solutions of chromium-doped titanium dioxide particles *J. Am. Chem. Soc.*, **104** 2996 (1982).
20. W. Choi, A. Termin, M. R. Hoffmann, The Role of Metal Ion Dopants in Quantum-Sized TiO<sub>2</sub>: Correlation between Photoreactivity and Charge Carrier Recombination Dynamics *J. Phys. Chem.*, **98**, 13669 (1994).
21. M. A. Henderson, J. M. White, H. Uetsuka, H. Onishi, Photochemical Charge Transfer and Trapping at the Interface between an Organic Adlayer and an Oxide Semiconductor *J. Am. Chem. Soc.*, **125**, 14974 (2003).
22. M. Anpo, M. Takeuchi, Design and development of second-generation titanium oxide photocatalysts to better our environment—approaches in realizing the use of visible light, *Int. J. Photoenergy*, **3**, 1 (2001).
23. M. Anpo, M. Takeuchi, *J. Catal.*, The design and development of highly reactive titanium oxide photocatalysts operating under visible light irradiation **216**, 505 (2003).
24. M. Futsuhara, K. Yoshioka, O. Takai, Optical properties of zinc oxynitride thin films, *Thin Solid Films*, **317** 322 (1998).
25. W. Choi, A. Termin, M. R. Hoffman, The Role of Metal Ion Dopants in Quantum-Sized TiO<sub>2</sub>: Correlation between Photoreactivity and Charge Carrier Recombination Dynamics *J. Phys. Chem.*, **98** 13669 (1994).
26. J. Wang, D. N. Tafen, J. P. Lewis, Z. Hong, A. Manivannan, M. Zhi, M. Li, N. Wu, Origin of Photocatalytic Activity of Nitrogen-Doped TiO<sub>2</sub> Nanobelts, *J. Am. Chem. Soc.*, **131** 12290 (2009).
27. S. S. Shinde, C. H. Bhosale, K. Y. Rajpure, Photocatalytic degradation of toluene using sprayed N-doped ZnO thin films in aqueous suspension, *J. Photochem. Photobiol. B, Biol.*, **113** 70 (2012).
28. V. Tiron, I.-L. Velicu, D. Stanescu, H. Magnan, L. Sirghi, High visible light photocatalytic activity of nitrogen-doped ZnO thin films deposited by HiPIMS, *Surf. Coat. Technol.*, **324** 594 (2017).